Image Features

A Comparison Between the Standard Hough Transform and the Mahalanobis Distance Hough Transform

Chengping Xu and Sergio A. Velastin

Department of Electronic and Electrical Engineering,
King's College London, University of London, Strand, London WC2R 2LS, England

Abstract. The Hough Transform is a class of medium-level vision techniques generally recognised as a robust way to detect geometric features from a 2D image. This paper presents two related techniques. First, a new Hough function is proposed based on a Mahalanobis distance measure that incorporates a formal stochastic model for measurement and model noise. Thus, the effects of image and parameter space quantisation can be incorporated directly. Given a resolution of the parameter space, the method provides better results than the Standard Hough Transform (SHT), including under high geometric feature densities. Secondly, Extended Kalman Filtering is used as a further refinement process which achieves not only higher accuracy but also better performance than the SHT. The algorithms are compared with the SHT theoretically and experimentally.

1 Introduction

The Hough transform is a many-to-one co-ordinate transformation from the *image space* **Z** to the *parameter space* **a**. The Standard Hough Transform (SHT) [1] is used to extract geometric features expressed by a single parametric equation such as:

$$\mathbf{f}(\mathbf{Z}_k, \mathbf{a}_i) = 0 \tag{1}$$

where the $\mathbf{Z}_k$ $(k = 1, \cdots, M_i)$, are the co-ordinate vectors of the image feature points (e.g. edge pixels) that make up a geometric feature ζ_i $(i = 1, \cdots, N)$ and $\mathbf{a}_i$ are the corresponding parameter vectors for ζ_i.

Generally, the aim is to find a subset of significant $\mathbf{a}_i$ from the superset of *all possible* $\mathbf{a}_i$, represented by a discrete "accumulator" array, through an *incrementation* or *voting* stage followed by an exhaustive *search* for maximum counts. The voting stage takes place through the computation of the Hough function

$$H(\mathbf{a}_i) = \sum_{k=1}^{M} I\left[\mathbf{f}(\mathbf{Z}_k, \mathbf{a}_i)\right] = \sum_{k=1}^{M} I\left[\mathbf{f}_i\right] \quad (i = 1, \cdots, N) \tag{2}$$

where M is the total number of image feature points. The *indication* function $I[\mathbf{f}_i]$ is defined by

$$I\left[\mathbf{f}_i\right] = \begin{cases} 1 & \mathbf{f}_i = 0 \\ 0 & \mathbf{f}_i \neq 0 \end{cases} \tag{3}$$

Lecture Notes in Computer Science, Vol. 800
Jan-Olof Eklundh (Ed.)
Computer Vision – ECCV '94

For example, straight line segments can be represented by the equation

$$\mathbf{f}(\mathbf{Z}_k, \mathbf{a}_i) = x_k \cos\theta_i + y_k \sin\theta_i - \rho_i \tag{4}$$

where $\mathbf{f} \in \Re^1$, $\mathbf{Z}_k = [x_k \quad y_k]^T \in \Re^2$ and $\mathbf{a}_i = [\theta_i \quad \rho_i]^T \in \Re^2$.

2 Advantages and Disadvantages of the SHT

The SHT has been shown particularly applicable in the presence of occlusion and missing or extraneous data (e.g. salt-and-pepper noise). Statistical tests [2] have shown the SHT to be more effective than alternative HT formulations. Although the evaluation of the indication function (Eqn. 3) has low computational cost, a large accumulator array (with a corresponding increase in computation time) is normally needed to achieve usable precision. Hence, a significant amount of research work has taken place in recent years [3, 4] to develop variants of the HT to address the conflict between high resolution and computational efficiency. Multiple resolution techniques or coarse-to-fine strategies [3, 5, 6] have been proposed, where high accumulator resolution is only used in places where a high density of votes accumulate. The main problem of such approaches is the potential undersampling of the Hough space. One important problem of the SHT is its degradation when there are errors in the co-ordinates of the image feature points [7]. This situation can arise due to digitisation noise, optical distortions or modelling inaccuracies, for which a number of stochastic approaches have been proposed [7, 8]. This paper presents two related techniques based on a Mahalanobis distance measure and Extended Kalman Filtering that incorporate a formal stochastic model for measurement and model noise.

3 The Mahalanobis Distance Hough Transform (MDHT)

3.1 Basic Principle

The geometric features of interest can be represented by the parametric equation

$$\mathbf{f}(\mathbf{Z}_k, \mathbf{a}_i) = 0 \tag{5}$$

where $\mathbf{f} \in \Re^p$, $\mathbf{Z}_k \in \Re^m$ and $\mathbf{a}_i \in \Re^n$. It is assumed that $\mathbf{Z}_k$ and $\mathbf{a}_i$ are independent zero-mean stochastic processes for which only estimate values of $\hat{\mathbf{Z}}_k$ and $\hat{\mathbf{a}}_i$ are available i.e.

$$E\left[\mathbf{Z}_k - \hat{\mathbf{Z}}_k\right] = 0, \qquad E\left[\left(\mathbf{Z}_k - \hat{\mathbf{Z}}_k\right)\left(\mathbf{Z}_k - \hat{\mathbf{Z}}_k\right)^T\right] = \mathbf{R}_k \tag{6}$$

$$E\left[\mathbf{a}_i - \hat{\mathbf{a}}_i\right] = 0, \qquad E\left[(\mathbf{a}_i - \hat{\mathbf{a}}_i)(\mathbf{a}_i - \hat{\mathbf{a}}_i)^T\right] = \mathbf{P}_i \tag{7}$$

where $\mathbf{R}_k$ is the *measurement* covariance matrix (related to image space resolution) and $\mathbf{P}_i$ is the *model* covariance matrix (related to parameter space resolution).

The voting stage of the Mahalanobis Distance Hough Transform (MDHT) takes place through the computation of the MD accumulating function

$$M(\hat{\mathbf{a}}_i) = \sum_{k=1}^{M} I\left[\mathbf{d}\left(\hat{\mathbf{Z}}_k, \hat{\mathbf{a}}_i\right)\right] = \sum_{k=1}^{M} I\left[\mathbf{d}_{ik}\right] \quad (i = 1, \cdots, N) \tag{8}$$

$$I\left[\mathbf{d}_{ik}\right] = \begin{cases} 1 & \mathbf{d}_{ik} \le \varepsilon \\ 0 & \mathbf{d}_{ik} > \varepsilon \end{cases} \tag{9}$$

where ε is a suitably chosen threshold to reject outliers (e.g. from a χ^2 distribution table), and the Mahalanobis Distance (MD) is given by

$$\mathbf{d}\left(\hat{\mathbf{Z}}_k, \hat{\mathbf{a}}_i\right) = \mathbf{d}_{ik} = \mathbf{f}\left(\hat{\mathbf{Z}}_k, \hat{\mathbf{a}}_i\right)^T \left\{ E\left[\mathbf{f}\left(\hat{\mathbf{Z}}_k, \hat{\mathbf{a}}_i\right) \mathbf{f}\left(\hat{\mathbf{Z}}_k, \hat{\mathbf{a}}_i\right)^T \right] \right\}^{-1} \mathbf{f}\left(\hat{\mathbf{Z}}_k, \hat{\mathbf{a}}_i\right) \tag{10}$$

The MD measure is thus an hypothesis test which measures the distance from the feature point to the contour mean (normalised by the target covariance matrix) and applies a threshold (ε) to determine if the point belongs to the contour. The authors have proposed a number of variants of the MDHT, fully described in [9, 10, 11].

3.2 Look-up Table Implementation of the MDHT

If the accumulator array represents constant parameter values, the MDHT can be executed off-line once over all possible image points, storing the results in a look-up table that can be regarded as containing a sequence of *templates*. The on-line MDHT thus becomes a search process of the corresponding parameter values for the feature points in an image. Matrix operations are replaced by template matching, saving considerable on-line computation time.

3.3 Extended Kalman Filter (EKF) Refinement

The accumulating cells represent candidate parameter values that can be further refined for higher accuracy and/or to reduce noise. The authors have investigated combinations of the MDHT and EKF [12] refinement in some detail [9-11], proposing two main methods: post-HT refinement (the EKF is applied on the peaks detected by the MDHT) and "integral" refinement (the EKF is applied as each image point is processed). These lead to reductions in the size of the accumulator array (modelled as parameter space quantisation noise) and sharper peaks that simplify the search stage. Due to space limitations, only post-HT refinement is discussed here.

4 Experimental Results

4.1 Typical Results

As an example, a typical real image (128×128), after conventional edge detection, is shown in Fig. 1. The centre of the image is chosen as the origin of the co-ordinate system. Fig. 2 shows the lines detected by the MDHT at fine parameter space resolution ($\Delta\theta = 2°, \Delta\rho = 2$) and superimposed on the original image. Table 1 shows a comparison of the results obtained for the MDHT with EKF refinement, and the MDHT for a coarse parameter space resolution of ($\Delta\theta = 10°, \Delta\rho = 5$), a reduction of

the size of the accumulator array by a factor of 12.5. These results illustrate that the MDHT/EKF combination does improve accuracy even for coarse resolutions. As the EKF is applied after peak detection, its accuracy improvement is limited by the accuracy of the MDHT (or any other HT).

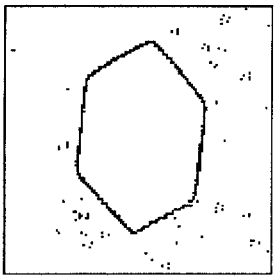

Fig. 1: Original edge image (128×128)

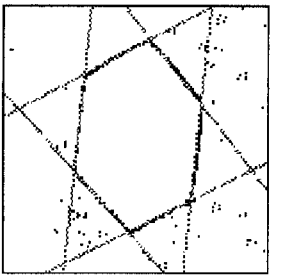

Fig. 2: Reconstructed image after the MDHT

Table 1. Comparison of accuracy between MDHT/EKF and MDHT

Real Values (θ,ρ)	$(\hat{\theta},\hat{\rho})$: MDHT/EKF	$(\hat{\theta},\hat{\rho})$: MDHT
(39.9, 37.0)	(39.92, 36.91)	(40, 35)
(119.1, 39.8)	(112.67, 39.10)	(110, 40)
(173.9, 28.0)	(177.45, 26.19)	(180, 25)
(223.2, 32.2)	(220.15, 31.04)	(220, 30)
(296.8, 38.3)	(293.31, 38.06)	(290, 40)
(353.0, 30.7)	(350.83, 30.26)	(350, 30)
Average Error	(3.12, 0.74)	(4.7, 1.6)

4.2 Statistical Performance Tests

The performance of the MDHT and MDHT/EKF algorithms presented here has been studied using the HT Test Framework developed by Hare and Sandler [2] which generates a large number of images with randomly distributed geometric features (e.g. position and length of straight lines). The same random sequence can be used to compare two or more different algorithms. The HT Test Framework measures parameter accuracy, detection (Det) and false alarm (FA) rates. The resolution used here is $\Delta\theta = 1.4^{o}, \Delta\rho = 1$. Fig. 3 shows Det and FA rates for the MDHT, the MDHT/EKF and the SHT (the SHT is the algorithm with best performance reported in [2]) using 12000 and 1200 images containing 1 to 20 lines. Extra one pixel error has been assigned to the co-ordinate system used by the MDHT and MDHT/EKF to test their sensitivity to errors in the variables.

Table 2 shows the effect of EKF refinement when applied after the MDHT using 200 images. Here, the co-ordinates in the SHT is also assigned the extra one pixel error. The improvement on the accuracy (represented by average errors) of parameter θ by the MDHT and the EKF is particularly noticeable.

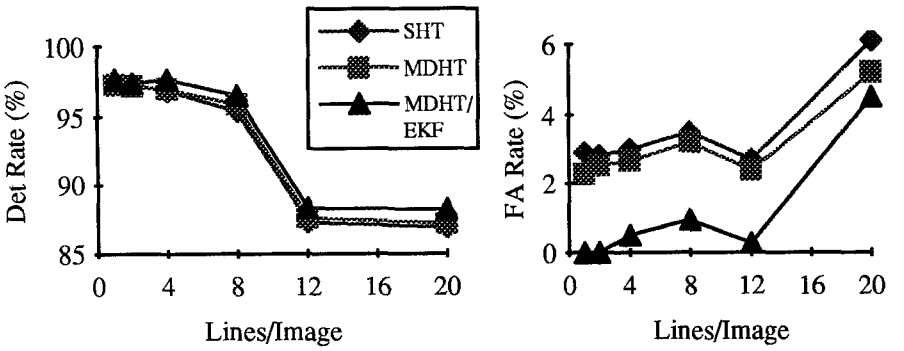

Fig. 3: Percentage detection rate and false alarm rate as a function of line density

Table 2: Parameter estimation errors by MDHT, MDHT/EKF and SHT

Lines	MDHT	MDHT/EKF	SHT
1	(0.402°, 0.703)	(0.069°, 0.673)	(0.414°, 0.678).
2	(0.406°, 0.722)	(0.074°, 0.685)	(0.430°, 0.706)
4	(0.400°, 0.706)	(0.098°, 0.696)	(0.431°, 0.704)
10	(0.413°, 0.707)	(0.139°, 0.701)	(0.453°, 0.701)

5 Conclusions

The combination of the MDHT and EKF refinement allows a coarser resolution of the parameter space than that of the SHT, hence storage savings can be significant. In principle, a coarser SHT can also be combined with EKF refinement. However, experimental results indicate that the MDHT has a higher line detection rate than the SHT, even when the density of lines in the image increases.

From the template matching point of view, the MDHT accumulating strategy can improve the shape of the stripe, as its hypothesis distance considers parameter and the measurement errors. The SHT accumulating function represents a true line only when the resolution of the parameters becomes extremely fine, but this might lead to voting spread due to oversampling.

Strictly speaking, the SHT can only be used in ideal cases when there are no parameter estimate and measurement errors. The MDHT algorithm presented here is more flexible than the SHT because both observation and estimation errors are accounted for. Thus, it can detect feature points in a predefined range around the contour, instead of just detecting feature points *exactly* on the contour as in the SHT. As shown through the use of the HT Test Framework, the MDHT combined with the EKF has better performance than the SHT even when working on dense images. This combination also allows reductions in the resolution of the accumulator array to obtain refined estimate results by a minimum mean square criterion with a corresponding reduction in processing time (e.g. compared to the usual least square methods).

Finally, the methods presented here are amenable to parallel processing (transputer implementations are currently under investigation) and therefore particularly attractive for dealing with real-world images in situations such as industrial inspection or vision-guided control.

6 Acknowledgements

The authors would like to thank Dr. A. Hare, Dr. M. Sandler and Mr. Hanif for their kindness and help. Also we would like to thank the IEE's Leslie H. Paddle Scholarship and the University of London Central Research Fund for their support.

References

1. R.O. Duda, P.E. Hart: Use of the Hough transform to detect lines and curves in pictures. Communications of the ACM 15, 11-15 (1972)
2. A.R. Hare, M.B. Sandler: General test framework for straight-line detection by Hough transforms. IEEE International Symposium on Circuits and Systems, 239-242 (1993)
3. J. Illingworth, J. Kittler: A survey of the Hough Transform. Computer Vision Graphics and Image Processing 44, 87-116 (1988)
4. V.F. Leavers: Which Hough transform? IEE Colloquium Digest on Hough Transform, Digest No. 1993/106 (1993)
5. J. Illingworth, J. Kittler: The adaptive Hough transform. IEEE Transactions on Pattern Analysis & Machine Intelligence 9 (5), 690-697 (1987)
6. M. Atiquzzaman: Multiresolution Hough transform—An efficient method of detecting patterns in images. IEEE Transactions on Pattern Analysis and Machine Intelligence 14 (11), 1090-1095 (1992)
7. N. Kiryati, A.M. Bruckstein: What's in a set of points. IEEE Transactions on Pattern Analysis & Machine Intelligence 14 (4), 496-500 (1992)
8. C.A. Darmon: A recursive method to apply the Hough transform to a set of moving objects. IEEE International Conference on Acoustics, Speech and Signal Processing, 825-829 (1982)
9. C. Xu: The Mahalanobis Hough Transform with Kalman Filter Refinement. MPhil Transfer Thesis, Internal Report No. 104/SCS/93, Department of Electronic and Electrical Engineering, King's College London, UK (1993)
10. C. Xu, S. A. Velastin: A Hough transform with integral Kalman filter refinement. IEE Colloquium Digest on Hough Transforms, Digest No. 1993/106, 4/1-4/4 (1993)
11. C. Xu, S. A. Velastin, A weighted mahalanobis distance Hough transform and its application for the detection of circular segments, IEE Colloquium Digest on Hough Transforms, Digest No. 1993/106, 3/1-3/4 (1993)
12. N. Ayache, O.D. Faugeras: Maintaining representations of the environment of a mobile robot. IEEE Transactions on Robotics and Automation 5(6), 804-819 (1989)